JOURNAL OF SPACECRAFT AND ROCKETS
Vol. 32, No. 5, September–October 1995

Deployment Mechanism for a Large Reflector: Thermal-Design Verification Using Flight Data

Akihiro Miyasaka,* Hiroaki Tsunoda,† and Katsuhiko Nakajima‡
NTT Wireless Systems Laboratories, Kanagawa 238-03, Japan

The thermal design of the deployment mechanism of a 3.5-m-diam reflector was certified using flight temperatures. The flight temperatures were recorded from Engineering Test Satellite Six, which was launched on Aug. 28, 1994, using an H-II vehicle. The satellite reflectors were successfully deployed on the sixth day after liftoff. The temperatures of the deployment mechanism and the difference in temperatures between the inner and the outer ring of the bearing for the deployment mechanism fell within the allowable temperature range. The minimum heating rate for the deployment mechanism was determined by taking into consideration the minimum allowable bearing temperature. The temperatures were evaluated using a thermal mathematical model of an antenna and a detailed model of the deployment mechanism. The antenna model was used to obtain boundary temperatures in the detailed model. This detailed model included the thermal contact resistance between the inner and the outer rings of the bearings. The predicted temperatures agreed with the flight data within 6%. The correct boundary temperatures are important in determining the exact temperature for the deployment mechanism. The thermal contact resistance between the inner and the outer ring was evaluated, considering the elastic deformation of the bearing due to the temperature difference between them. The thermal resistance in the flight agreed well with the value estimated in the ground tests.

Introduction

FUTURE communication systems will use advanced communication satellites that offer increased communication capacity by covering the service area with multiple-spot beams. Engineering Test Satellite Six (ETS-VI) was launched on Aug. 28, 1994, using an H-II vehicle to evaluate several new technologies. The main onboard antenna system included large deployable reflectors with aperture diameters of 3.5 and 2.5 m for forming spot beams.[1] Two large deployable reflectors were launched folded up for efficient storage and were extended in orbit. The stowed and deployed antenna system configurations are shown in Figs. 1 and 2, respectively. The two main reflectors were constructed from honeycomb sandwich panels of carbon-fiber-reinforced plastics (CFRPs) with CFRP trusses as the support structure to achieve large and lightweight reflectors. The reflector surfaces were coated with white paint, which had a low absorption [0.25 at beginning of launch (BOL)] and a high emission (0.82 at BOL). The truss structure was covered with multilayer insulation (MLI) blankets to shade it from the sun's rays. To stabilize the antenna temperature, the ETS-VI reflectors were deployed while facing the sun. Antenna deployment started with the deployment of the wings to form the 3.5-m-diam reflector. The reflector was deployed by a mechanism fixed to the central tower. The 2.5-m reflector was then deployed.

Space-qualified bearings were used in the deployment mechanisms to position the reflectors and form their surfaces. The parameters for the beam-pointing accuracy of each reflector were used to determine the maximum specified temperature difference between the inner and the outer bearing rings.[2] As the 3.5-m-diam reflector required the highest level of pointing accuracy, its temperature-difference requirement was the strictest of all the bearings.

The bearings for the 3.5-m reflector were space-qualified deep-groove ball bearings. The maximum temperature difference between the inner and outer rings was set at 25°C for structural reasons. If the temperature difference exceeded this specification, the beam pointing accuracy could not be guaranteed, and the reflector deployment would be unreliable. The predicted temperatures of the deployment mechanism for the 3.5-m-diam reflector were calculated by considering the thermal resistance between the inner and the outer bearing rings.

Temperatures over the entire antenna system had been predicted using an approximately 300-element thermal mathematical model and verified through thermal balance testing on the ground.[3] Heaters and MLI blankets were applied to the deployment mechanism to keep temperatures within the allowable range. However, since sensors could not be placed on the inner and the outer ring because they

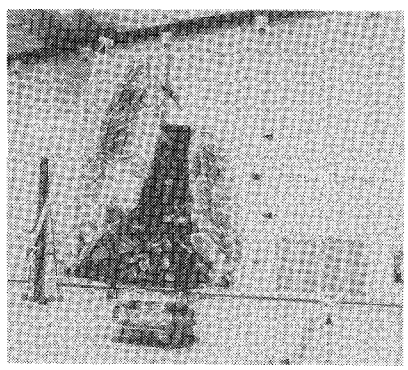

Fig. 1 Stowed antenna part.

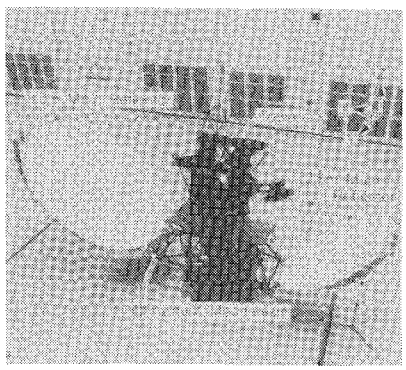

Fig. 2 Deployed antenna part.

Received Nov. 29, 1994; revision received April 20, 1995; accepted for publication April 28, 1995.

*Research Engineer, Satellite Communication Systems Laboratory, 1-2356, Take Yokosuka-shi. Member AIAA.
†Senior Research Engineer. Member AIAA.
‡Senior Research Engineer, Supervisor. Member AIAA.

would prevent rotation, they were placed near the rings. As a result, the temperatures of the rings had to be estimated from the sensor readings.

This paper describes the method used to predict temperatures of the deployment mechanism for a 3.5-m-diam reflector and a comparison of the predicted and flight data.

Deployment Mechanism

The deployment mechanism of the 3.5-m-diam reflector is shown in Fig. 3. Figures 3a and 3b show the conditions before and after reflector deployment, respectively. The deployment mechanism with the MLI blankets is shown in Fig. 4. This figure depicts the configuration for a half-open reflector. The inner ring holds a shaft attached to the main reflector; the outer ring is mounted to the chassis of the tower; the latch mechanism that locks the reflector when extended is connected to the chassis; the bearing, the arm, and the chassis are covered with MLI blankets to isolate the deployment mechanism, but the latch mechanism is exposed to space. Although the arm and chassis are made of aluminum alloys, the latch parts of the deployment mechanism are constructed of titanium in order to prevent any loss of antenna-pointing accuracy due to thermal and latch-impact distortions.

The bearing rings and ball and are made of stainless steel. The roughness of the contact surface is less than 0.5×10^{-6} m, so the surface was regarded as smooth. The force generated by a coil spring was considered to be in the axial direction. There are seven balls in each bearing, and heat transfer from the outer to the inner ring was assumed to occur through the balls.

Prior to reflector extension, the solar rays struck the MLI of the 2.5-m reflector. The heat was transferred by conduction to the deployment mechanism through the reflector and by radiation from the tower. For the 3.5-m reflector, the only areas exposed to solar radiation were the edges of the side wings. Thus, the amount of heat conduction from reflector to deployment mechanism was small for the 3.5-m reflector. The radiation effect from the tower was also small, because of the shading offered by the tower's MLI blankets. Consequently, the deployment mechanism of the 3.5-m reflector was almost totally shaded, so that its temperature was very low. Therefore, we had to control the temperature of the deployment mechanism with electric heaters.

Since the inner ring had to be rotated for reflector extension, temperature sensors could not be directly attached to the rings. Instead, they were attached near the rings: the inner-ring sensor at the center of the arm, and the outer-ring sensor between the tower boundary and the arm. The inner- and outer-ring temperatures were estimated from the sensor temperatures.

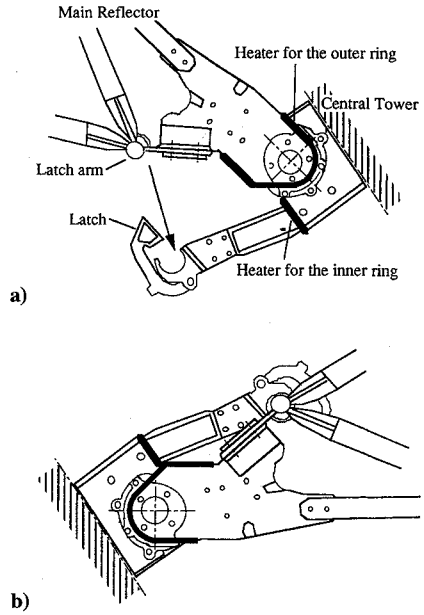

Fig. 3 Condition a) before and b) after reflector deployment.

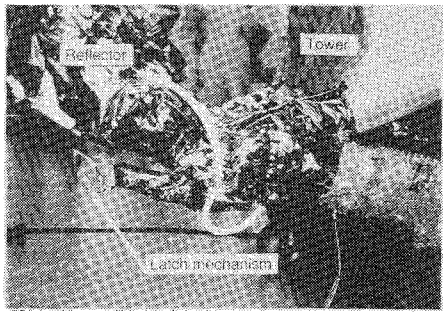

Fig. 4 Deployment mechanism with MLI.

Thermal Mathematical Model

A thermal mathematical model was made for the antenna system and for the deployment mechanism. The antenna model consisted of approximately 300 analysis elements.[3] The antenna model, in a stowed configuration, is shown in Fig. 5. It consisted of rectangular, triangular, spherical, cylindrical, elliptical, and circular cone shapes. This model was used to predict roughly whether or not all antenna temperatures lay within the allowable temperature range. Moreover, the antenna temperatures were entered into the detailed model so that temperatures such as those of the bearings could be put under closer scrutiny. Because the temperature difference between the prediction and allowable minimum temperature was small, the detailed model was used to estimate the temperatures of the inner and the outer bearing rings. The tower and the reflectors in the antenna model were used as boundaries of the deployment-mechanism analysis model. The temperatures of the antenna model were obtained using NEVADA^{TM} and SINDA^{TM} software packages.

The detailed deployment-mechanism model was divided into 22 elements and included the thermal contact resistance between the inner and the outer bearing rings. The thermal resistance of the bearing parts consists of the contact resistance between the balls and the inner and outer rings, and between the deployment mechanism and the inner and the outer rings. The latter contribution can be calculated because the part size, the contact area, and the thermal conductivity are known. However, it is difficult to obtain the former contribution, because the contact area between the ball and the inner or the outer ring depends on the part deformation caused by the coil spring. This contact resistance accounts for over 80% of the total bearing heat transfer, so accurately estimating it is extremely important. The thermal resistance across a joint consisting of solid or hollow metallic bodies in elastic contact with two smooth plates has been discussed.[4–6] In this study, the thermal resistance was evaluated on the basis of Ref. 4. Heat transfer across the bearing occurred via conduction through the balls and between the elements via radiation. The latter heat flux, however, is so small that it was neglected.[4]

The following four assumptions are made to estimate the thermal resistance: 1) heat transfer occurs through contact conduction; 2) the surface is so smooth that the elasticity theory for the contact area, i.e., the Hertzian theory,[4–6] is applicable; 3) since the heat flow pattern in the contacting elements is approximated as symmetrical over the contact area, the contact area is isothermal; and 4) the temperature far from the contact area is uniform.

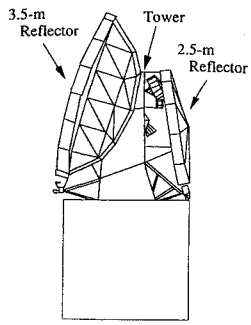

Fig. 5 Thermal mathematical model of antenna.

The thermal resistance is estimated as follows. Temperatures of the antenna system are used as the boundary temperatures for the detailed model of the deployment mechanism. The resistance between the inner ring and the balls and the resistance between the balls and the outer ring are substituted as the initial values. The radius of the contact ellipse formed through thermal expansion is calculated after estimating the bearing temperatures. The eccentricity of the contact ellipse is obtained from a contact-ellipse equation, and the exact contact angle is calculated by summing the displacements of the contacting solids. The resistance between the inner ring and the balls and that between the balls and the outer ring are updated, and finally the procedures are iterated using the updated resistance of both until convergence is achieved.

Determining Heat Generation Rate

Heaters are used to keep the temperature of the deployment mechanism within the allowable range. Because of the space and power constraints of the satellite, it was decided to let the temperature of the deployment mechanism approach the minimum allowable value. The amount of heat applied to the mechanism is determined from two factors: the minimum bearing temperature and the positive bearing clearance. The latter is achieved by ensuring that the inner bearing is always colder than the outer ring.

Two heaters were used to control the inner and outer ring temperatures. The heater attachment areas were very small. The heater for the outer ring was attached to the chassis, close to the tower interface. The heater for the inner ring was attached to the arm part located at the end of the shaft. The amount of power supplied to the heaters was evaluated using the detailed thermal mathematical model for the deployment mechanism, taking into consideration the thermal contact resistance between the inner and the outer ring of the bearing. Calculations were done taking into consideration the steady state of the stowed antenna in a solar cruising mode.

The inner- and outer-ring heaters, respectively, consumed 0.3 and 0.1 W, taking into consideration the minimum allowable bearing temperature of −70°C. Although the stated outer-ring temperature was higher than the inner-ring, temperature, the heat generation rate of the inner-ring heater was greater than that of the outer-ring heater. The reason for this was that the temperature of the reflector boundary for the inner ring was lower than that of the tower boundary for the outer ring. The temperature of the tower obtained from the antenna model was −65°C. The temperature of the reflector was −73°C. The temperatures of the inner ring and the outer ring were within the allowable range. In addition, the difference between the inner and the outer temperature was within the allowable range.

Verification of Thermal Design in Deployment Mechanism

The reflectors were successfully deployed on the sixth day after liftoff. The temperatures of the antenna system reached equilibrium about 50 h after liftoff, so that reflector deployment occurred under steady-state conditions. The predicted and flight temperature data are compared in Fig. 6. At approximately 80 h after liftoff, there was a sudden spike in temperatures due to a change in satellite attitude. While the flight temperatures fell rapidly after liftoff, the predicted temperatures fell more slowly, and the difference is thought to be caused by inaccurate estimation of the heat capacity of the deployment mechanism. It was especially difficult to estimate the heat capacity of the MLI, because of the complex shape of the deployment mechanism. However, the temperatures of the deployment mechanism fell within the allowable range. The difference in temperatures measured by the two sensors for the inner and the outer deployment mechanism shown in Fig. 3 was very small, about 3°C. We obtained this value on the basis of the fact that the difference in temperature between the sensor element inside and that of the one outside was always smaller than the difference between the inner and the outer ring. Therefore, this result shows that the thermal design for the deployment mechanism was very effective and successful.

Comparison Between Predicted and Flight Data

The relationship between the predicted temperatures and sensor temperatures in a steady state is shown in Table 1. The temperature

Table 1 Comparison between prediction and flight data

	Temperature, °C			
	$-Y$ side		$+Y$ side	
	Prediction	Flight data	Prediction	Flight data
Sensor near outer ring	−62	−66	−59	−66
Sensor near inner ring	−64	−68	−58	−64
Outer ring	−61	—	−57	—
Inner ring	−62	—	−58	—

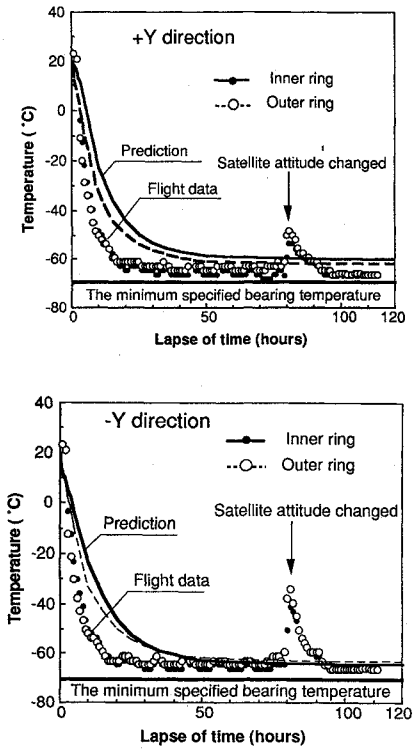

Fig. 6 Comparison between prediction and flight data for the deployment mechanism.

of the inner ring must be kept lower than that of the outer ring in order to maintain the bearing's design clearance. As the sensors could not be attached to rings directly, their flight data could not be compared with the analysis results. However, the temperatures were measured for the sensors attached near the inner and the outer ring.

Based on the analysis results, we estimated the temperatures of the inner ring to be lower than those of the outer rings. In the $-Y$ direction, the temperature of the sensor near the inner ring was lower than that near the outer ring, as shown in Table 1. The predicted temperatures agreed with flight data within a 6% deviation.

In contrast, from the in-flight data and analysis results it can be seen that in the $+Y$ direction, the temperature near the inner ring is higher than that for the sensor near the outer ring. However, the analysis models indicate that the inner ring was actually colder than the outer ring despite.

Improvement of Analysis Temperatures for Deployment Mechanism

The difference in temperature between the predicted and flight data for the deployment mechanism was on average about 4°C, with a maximum value of 6°C. This result shows that the thermal design and the thermal analysis model are effective enough. The difference can be ascribed to the level of accuracy in the boundary temperatures obtained from the antenna model. The thermal conductance in the antenna model was confirmed through thermal-balance testing on the ground. However, the accuracy can be enhanced by increasing the number of antenna model elements. The tower and the reflector

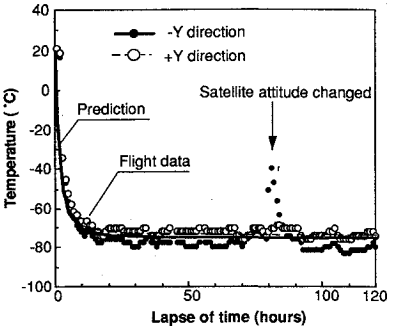

Fig. 7 Comparison between predicted and flight data for the interface.

interface temperatures were used as boundary temperatures to predict the temperature of the deployment mechanism. Since the sensors could not be attached to all the required interfaces on account of the limited number of telemetry command channels available, only the flight temperature for the reflector interface was obtained. The tower interface temperature was predicted from the antenna system model. Figure 7 shows the predicted temperatures using boundary conditions from the antenna model, which were about 3°C higher than the flight data. The flight temperatures, however, were used for the interfaces. The average difference between the predicted and flight temperatures for the deployment mechanism was about 2°C.

Thermal Contact Resistance of the Bearing

The thermal contact resistance between the inner and the outer bearing rings was estimated from the flight data. The thermal contact resistance depends upon the contact angle, and it is possible for the contact angle to change in space because of thermal expansion. The nominal contact angle was taken to be 15 deg. Though it was impossible to measure the contact angle in space directly, it was estimated using the flight temperatures on the deployment mechanism. We express the contact angle as a function of the bearing shape, i.e., the sizes of the inner ring, the outer ring, and the ball, and the clearances between the ball and the two rings. An equation for the clearances is obtained by taking into consideration the external force and the elastic deformation of the bearing using the flight temperatures for the deployment mechanism. Therefore, the in-flight thermal contact resistance was obtained from the deployment-mechanism temperatures.

The thermal resistance for the flight-qualified bearing was 48.599 K/W, obtained in ground tests. The tests indicated that the axial force generated by a spring acting on the inner ring was 14 N. In flight, the thermal resistance calculated using the deployment mechanism temperatures was 48.597 K/W. The two thermal resistances are nearly equal. A small temperature difference of approximately 1°C occurred between the inner and the outer ring. The degree of elastic deformation from the thermal expansion was very low. Therefore, the design value of the thermal resistance was sufficiently accurate.

Conclusion

The thermal design for the deployment mechanism of a 3.5-m-diam reflector was certified using flight temperatures. The temperatures were evaluated using the antenna model and a detailed model of the deployment mechanism. The antenna model was used to obtain the interface temperatures which were used in the detailed model. Inasmuch as the temperatures of the deployment mechanism as well as the temperature difference between the inner and outer bearing rings did not exceed the allowable ranges, the thermal design was considered useful and effective. In addition, the thermal resistance of the bearing was estimated from the flight temperatures of the deployment mechanism. Since the in-flight temperature difference between the inner and the outer ring was small, the thermal contact resistance of the two rings was equivalent to that in the ground test results. Thus, this thermal deployment-mechanism design achieved the deployment of the large reflector.

References

[1]Ohtomo, I., and Kumazawa, H., "Development of the On-Board Fixed and Mobile Multi-Beam Antenna for ETS-VI Satellite," AIAA Paper 90-0805, March 1990.

[2]Kawakami, Y., Hojo, H., and Ueba, M., "Analysis of an On-Board Antenna Pointing Control System," *Journal of Guidance, Control, and Dynamics*, Vol. 13, No. 4, 1990, pp. 762, 763.

[3]Tsunoda, H., Nakajima, K., and Miyasaka, A., "Thermal Design Verification of Large Deployable Antenna for a Communications Satellite," *Journal of Spacecraft and Rockets*, Vol. 29, No. 2, 1992, pp. 271–278.

[4]Nakajima, K., "Thermal Contact Resistance Between Balls and Rings of a Bearing Under Axial, Radial and Combined Loads," *Journal of Thermophysics and Heat Transfer*, Vol. 9, No. 1, 1995, pp. 88–95.

[5]Yovanovich, M. M., "Thermal Constriction Resistance Between Contacting Metallic Paraboloids: Application to Instrument Bearings," AIAA Paper 70-857, June–July 1970.

[6]Yovanovich, M. M., and Schneider, G. E., "Thermal Constriction Resistance Due to a Circular Annular Contact," AIAA Paper 76-142, Jan. 1976.

T. E. Vas
Associate Editor